Available online at www.sciencedirect.com
ScienceDirect
Journal of Sound and Vibration 299 (2007) 212–228
JOURNAL OF SOUND AND VIBRATION
www.elsevier.com/locate/jsvi

Dynamic responses of Reissner–Mindlin plates with free edges resting on tensionless elastic foundations

L. Yu[a], Hui-Shen Shen[a,b,*], X.-P. Huo[a]

[a]*School of Ocean and Civil Engineering, Shanghai Jiao Tong University, Shanghai 200030, People's Republic of China*
[b]*State Key Laboratory of Ocean Engineering, Shanghai Jiao Tong University, Shanghai 200030, People's Republic of China*

Received 2 August 2005; received in revised form 30 June 2006; accepted 10 July 2006
Available online 25 September 2006

Abstract

Dynamic response analysis is presented for a Reissner–Mindlin plate with four free edges resting on a tensionless elastic foundation of the Winkler-type and Pasternak-type. The mechanical loads consist of transverse partially distributed impulsive loads and in-plane static edge loads while the temperature field is assumed to exhibit a linear variation through the thickness of the plate. The material properties are assumed to be independent of temperature. The two cases of initially compressed plates and of initially heated plates are considered. The formulations are based on Reissner–Mindlin first-order shear deformation plate theory and include the plate–foundation interaction and thermal effects. A set of admissible functions is developed for the dynamic response analysis of moderately thick plates with four free edges. The Galerkin method, the Gauss–Legendre quadrature procedure and the Runge–Kutta technique are employed in conjunction with this set of admissible functions to determine the deflection-time and bending moment–time curves, as well as shape mode curves. An iterative scheme is developed to obtain numerical results without using any assumption on the shape of the contact region. The numerical illustrations concern moderately thick plates with four free edges resting on tensionless elastic foundations of the Winkler-type and Pasternak-type, from which results for conventional elastic foundations are obtained as comparators. The results confirm that the plate will have stronger dynamic behavior than its counterpart when it is supported by a tensionless elastic foundation.

1. Introduction

The analysis of plates on elastic foundations have been motivated by the need in engineering to design, for example, mat and raft foundations, pavement slabs of roads and airfield. These problems are usually analyzed by assuming that the foundation reacts in compression as well as in tension [1]. This assumption that the contact between the plate and its support is established continuously simplifies the problem. However, it is well known that in many practical cases, this assumption is questionable. Some supporting media cannot sometimes provide tensile reaction and, under certain conditions, some portions of the plate may lift-off. Therefore, a tensionless foundation, where the reaction is only compressive, is modelled. The plates resting on

*Corresponding author.
E-mail address: hsshen@mail.sjtu.edu.cn (H.-S. Shen).

0022-460X/$ - see front matter © 2006 Elsevier Ltd. All rights reserved.
doi:10.1016/j.jsv.2006.07.015

a tensionless foundation is complicated because the location and extent of the contact regions are not known at the outset. Since the stresses and deformations of the plate and foundation depend on the contact area and therefore on its unknown boundaries, these boundaries are, along with other mechanical quantities, part of the solution, being the primary unknowns of the problem. So, even for cases involving linear foundation models and linear plate theories, the problem is nonlinear by virtue of unilateral constraints and therefore needs to be solved iteratively.

Many linear bending studies for thin and moderately thick, circular and rectangular plates resting on a tensionless elastic foundation are available in the literature see, for example, Refs. [2–13]. They concluded that the contact region remains constant and is independent of the load level. In contrast, Khathlan [14] and Hong et al. [15] studied the large deflections of circular plates resting on a tensionless elastic foundation of the Winkler-type and concluded that as the transverse load increases the contact area tends to expand until full contact is reached. Recently, Guler [16] presented a bending analysis for a thin circular plate subjected to concentrated central and distributed loads and resting on a tensionless elastic foundation of the Pasternak-type. Also recently, Shen and Yu [17] gave a nonlinear bending analysis for a rectangular plate with four free edges subjected to thermomechanical loads and resting on a tensionless elastic foundation of the Pasternak-type. In this study, the formulations were based on the first-order shear deformation plate theory and the effect of initial in-plane compressive load and initial temperature variation on the nonlinear bending behavior was reported. However, the dynamic analysis for a plate resting on tensionless elastic foundations is limited in number. Celep and Turhan [18], and Guler and Celep [19], and Celep and Guler [20] studied, respectively, the dynamic responses of flexible and rigid circular plates subjected to time dependent external moment and/or transverse loads and resting on a tensionless elastic foundation of the Winkler-type. They concluded that the extent of the contact region and deflections of the plate depending on the loading combination and on time. However, in their studies the formulations were based on the Kirchhoff–Love hypothesis and therefore the transverse shear deformations were not accounted for. To the best of the authors' knowledge, there is no literature covering dynamic response of shear deformable rectangular plates resting on a tensionless elastic foundation of Pasternak-type.

The present study extends the previous works [1,17] to the case of moderately thick rectangular plates with four free edges resting on a tensionless elastic foundation of the Pasternak-type. It is worth to note that in the case of two-parameter foundation model there are two different types of boundary conditions for partial contact and complete contact [21]. For the complete contact, a boundary force appears as a result of the second parameter of the foundation, whereas in the case of partial contact there is no boundary force like that. Therefore, only the partial contact case is considered in the present study. In such a case the plate may lift off the foundation and no boundary force occurs. The mechanical loads consist of transverse partially distributed impulsive loads and in-plane static edge loads while the temperature field is assumed to exhibit a linear variation through the thickness of the plate. The material properties are assumed to be independent of temperature. The two cases of initially compressed plates and of initially heated plates are considered. The formulations are based on Reissner–Mindlin first-order shear deformation plate theory and include the plate–foundation interaction and thermal effects. A set of admissible functions, which satisfy both geometrical and natural boundary conditions, are developed for the dynamic responses analysis of moderately thick plates with four free edges. The Galerkin method, the Gauss–Legendre quadrature procedure and the Runge–Kutta technique are employed in conjunction with this set of admissible functions to determine the deflection-time and bending moment–time curves, as well as shape mode curves. An iterative scheme is developed to obtain numerical results without using any assumption on the shape of the contact region. Numerical results are presented in dimensionless graphical form to illustrate the effect of the tensionless character of the foundation.

2. Analytical formulations

Consider a rectangular thick plate with four free edges of length a, width b and thickness h, which rests on, but is not attached to, a tensionless elastic foundation. Let X, Y and Z be a set of coordinates with X and Y axes located in the middle plane of the plate and the Z axis pointing downwards. The origin of the coordinate system is located at the center of the plate in the middle plane. The plate is exposed to a stationary temperature field $T(X, Y, Z)$ and/or transverse dynamic patch load $q(\bar{t})$ in the shaded region, as shown in Fig. 1, combined

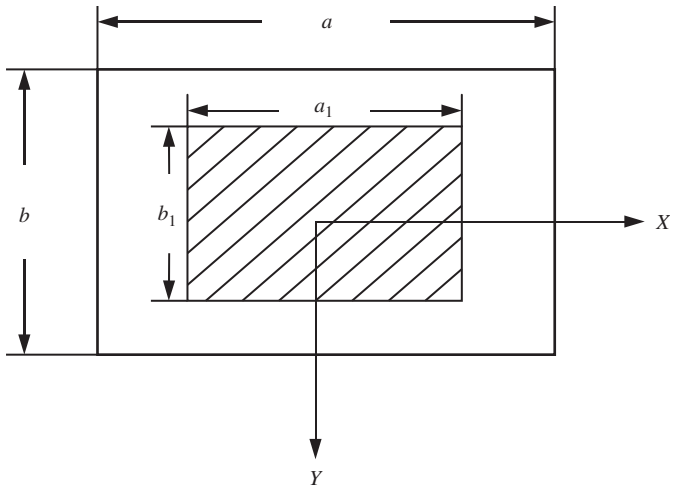

Fig. 1. Rectangular plate subjected to a partially distributed impulsive load.

with in-plane static edge loads P_x in the X-direction and P_y in the Y-direction. The components of displacement of the middle surface along the X, Y and Z axes are designated by $\bar{U}$, $\bar{V}$ and $\bar{W}$. $\bar{\Psi}_x$ and $\bar{\Psi}_y$ are the mid-plane rotations of the normals about the Y and X axes, respectively. The foundation is represented by a two-parameter foundation model, that is, the reaction of the foundation is assumed to be $p = \bar{K}_1\bar{W} - \bar{K}_2\nabla^2\bar{W}$, where p is the force per unit area, $\bar{K}_1$ is the Winkler foundation stiffness, $\bar{K}_2$ is a constant showing the effect of the shear interactions of the vertical elements, ∇^2 is the Laplace operator in X and Y. This reaction, however, is only compressive and occurs only where p is positive. Let $\bar{F}$ (X, Y) be the stress function for the stress resultants defined by $\bar{N}_x = \bar{F}_{,yy}$, $\bar{N}_y = \bar{F}_{,xx}$ and $\bar{N}_{xy} = -\bar{F}_{,xy}$, where a comma denotes partial differentiation with respect to the corresponding coordinates.

From Reissner–Mindlin plate theory considering the first-order shear deformation effect, including plate–foundation interaction and thermal effects, the equations of motion of such plates are

$$\tilde{L}_{11}(\bar{\Psi}_x) + \tilde{L}_{12}(\bar{\Psi}_y) + \tilde{L}_{13}(\bar{W}) + \tilde{L}_{14}(\bar{W}) + H(\bar{W})[\bar{K}_1\bar{W} - \bar{K}_2\nabla^2\bar{W}] + \nabla^2\bar{M}^{\mathrm{T}} = q, \tag{1}$$

$$\tilde{L}_{21}(\bar{\Psi}_x) + \tilde{L}_{22}(\bar{\Psi}_y) + \tilde{L}_{23}(\bar{W}) + \tilde{L}_{24}(\bar{\Psi}_x) + (\bar{M}^{\mathrm{T}})_{,x} = 0, \tag{2}$$

$$\tilde{L}_{31}(\bar{\Psi}_x) + \tilde{L}_{32}(\bar{\Psi}_y) + \tilde{L}_{33}(\bar{W}) + \tilde{L}_{34}(\bar{\Psi}_y) + (\bar{M}^{\mathrm{T}})_{,y} = 0, \tag{3}$$

$$\nabla^4\bar{F} + (1-\nu)\nabla^2\bar{N}^{\mathrm{T}} = 0. \tag{4}$$

Because the plate is not attached to the foundation, tensile stresses cannot occur between plate and foundation and therefore the plate may lift off the foundation over certain intervals. In the case of partial contact, no concentrated edge reactions occur as reported in Ref. [21], and a compressive reaction arises when there is contact between the plate and the foundation, no reaction comes into being when a separation develops. This character of the foundation is taken into account by introducing a contact function defined by

$$H(\bar{W}) = \begin{cases} 1 & \text{for} \quad p = \bar{K}_1\bar{W} - \bar{K}_2\nabla^2\bar{W} > 0, \\ 0 & \text{for} \quad p = \bar{K}_1\bar{W} - \bar{K}_2\nabla^2\bar{W} \leqslant 0, \end{cases} \tag{5}$$

and the linear operators $\tilde{L}_{ij}()$ are defined by

$$\tilde{L}_{11}() = -\kappa^2 Gh\frac{\partial}{\partial X}, \quad \tilde{L}_{12}() = -\kappa^2 Gh\frac{\partial}{\partial Y},$$

$$L_{13}() = -\left[\left(\kappa^2 Gh + N_X\right)\frac{\partial^2}{\partial X^2} + \left(\kappa^2 Gh + N_Y\right)\frac{\partial^2}{\partial Y^2}\right],$$

$$\tilde{L}_{21}() = \kappa^2 Gh - D\left(\frac{\partial^2}{\partial X^2} + \frac{1-v}{2}\frac{\partial^2}{\partial Y^2}\right), \quad \tilde{L}_{23}() = \kappa^2 Gh\frac{\partial}{\partial X},$$

$$\tilde{L}_{31}() = \tilde{L}_{22}() = -\frac{1+v}{2}D\frac{\partial^2}{\partial X \partial Y}, \quad \tilde{L}_{32}() = \kappa^2 Gh - D\left(\frac{1-v}{2}\frac{\partial^2}{\partial X^2} + \frac{\partial^2}{\partial Y^2}\right),$$

$$\tilde{L}_{33}() = \kappa^2 Gh\frac{\partial}{\partial Y}, \quad \tilde{L}_{14}() = I_1\frac{\partial^2}{\partial \bar{t}^2}, \quad \tilde{L}_{24}() = \tilde{L}_{34}() = I_3\frac{\partial^2}{\partial \bar{t}^2},$$

$$\nabla^2() = \frac{\partial^2}{\partial X^2} + \frac{\partial^2}{\partial Y^2}, \quad \nabla^4() = \frac{\partial^4}{\partial X^4} + 2\frac{\partial^4}{\partial X^2 \partial Y^2} + \frac{\partial^4}{\partial Y^4}, \tag{6a}$$

where

$$(I_1, I_3) = \int_{-h/2}^{h/2} \rho(1, Z^2)\,\mathrm{d}Z, \tag{6b}$$

and D is flexural rigidity and $D = Eh^3/[12(1-v^2)]$. E is Young's modulus, G is the shear modulus and v is Poisson's ratio. Also κ^2 is the shear factor, which accounts for the non-uniformity of the shear strain distribution through the plate thickness. For Reissner plate theory $\kappa^2 = 5/6$, while for Mindlin plate theory $\kappa^2 = \pi^2/12$.

If all four edges of the plate are free, for the partial contact case, the boundary conditions are

$X = \pm a/2$:

$$\bar{M}_x = D\left(\frac{\partial \bar{\Psi}_x}{\partial X} + v\frac{\partial \bar{\Psi}_y}{\partial Y}\right) - \bar{M}^{\mathrm{T}} = 0, \tag{7a}$$

$$\bar{M}_{xy} = \frac{1-v}{2}D\left(\frac{\partial \bar{\Psi}_x}{\partial Y} + \frac{\partial \bar{\Psi}_y}{\partial X}\right) = 0, \tag{7b}$$

$$\bar{Q}_x = \kappa^2 Gh\left(\bar{\Psi}_x + \frac{\partial \bar{W}}{\partial X}\right) = 0, \tag{7c}$$

$$\int_{-b/2}^{+b/2} \bar{N}_x\,\mathrm{d}Y + \sigma_x bh = 0, \tag{7d}$$

$Y = \pm b/2$:

$$\bar{M}_y = D\left(v\frac{\partial \bar{\Psi}_x}{\partial X} + \frac{\partial \bar{\Psi}_y}{\partial Y}\right) - \bar{M}^{\mathrm{T}} = 0, \tag{7e}$$

$$\bar{M}_{xy} = \frac{1-v}{2}D\left(\frac{\partial \bar{\Psi}_x}{\partial Y} + \frac{\partial \bar{\Psi}_y}{\partial X}\right) = 0, \tag{7f}$$

$$\bar{Q}_y = \kappa^2 Gh\left(\bar{\Psi}_y + \frac{\partial \bar{W}}{\partial Y}\right) = 0, \tag{7g}$$

$$\int_{-a/2}^{+a/2} \bar{N}_y\mathrm{d}X + \sigma_y ah = 0, \tag{7h}$$

where σ_x and σ_y are the average compressive stresses in the X- and Y-directions, $\bar{M}_x$ and $\bar{M}_y$ are the bending moments per unit width and per unit length of the plate, and $\bar{Q}_x$ and $\bar{Q}_y$ are the transverse shear forces, respectively.

For the initially heated plate, it is assumed that $\sigma_x = \sigma_y = 0$ and the temperature field is assumed to be a linear variation through the plate thickness, i.e.

$$T(X, Y, Z) = T_0\left[1 + C\frac{Z}{h}\right], \tag{8}$$

in which T_0 and C denote the temperature amplitude and gradient, respectively.

The thermal force and moments caused by the temperature field $T(X, Y, Z)$ are defined by

$$(\bar{N}^{\mathrm{T}}, \bar{M}^{\mathrm{T}}) = \frac{E\alpha}{1-\nu}\int_{-h/2}^{+h/2}(1, Z)T(X, Y, Z)\,\mathrm{d}Z, \tag{9}$$

where α is the thermal expansion coefficient of a plate.

Because of Eqs. (8) and (9), it is noted that the temperature does not vary in X and Y, then thermal force $\bar{N}^{\mathrm{T}}$ and moment $\bar{M}^{\mathrm{T}}$ are constants, so that the boundary conditions of Eqs. (7a) and (7e) are non-homogeneous, but in Eqs. (1)–(4) $\nabla^2\bar{M}^{\mathrm{T}} = \nabla^2\bar{N}^{\mathrm{T}} = (\bar{M}^{\mathrm{T}})_{,x} = (\bar{M}^{\mathrm{T}})_{,y} = 0$.

For the initially compressed plate, it is assumed that $\bar{N}^{\mathrm{T}} = \bar{M}^{\mathrm{T}} = 0$, now the boundary conditions of Eqs. (7a) and (7e) become homogeneous.

3. Analytical method and solution procedure

Before proceeding, it is convenient first to define the following dimensionless quantities for such plates (in which the alternative forms k_1 and k_2 are not needed until the numerical examples are considered)

$$\begin{aligned}
&x = \pi X/a, \quad y = \pi Y/b, \quad \beta = a/b, \quad \gamma = \pi^2 D/a^2\kappa^2 Gh, \quad (\nu_1, \nu_2) = (1-\nu, 1+\nu)/2,\\
&W = \bar{W}[12(1-\nu^2)]^{1/2}/h, \quad (\Psi_x, \Psi_y) = (\bar{\Psi}_x, \bar{\Psi}_y)a[12(1-\nu^2)]^{1/2}/\pi h,\\
&F = \bar{F}/D, \quad (Q_x, Q_y) = (\bar{Q}_x, \bar{Q}_y)a[12(1-\nu^2)]^{1/2}/\pi\kappa^2 Gh^2, \quad \theta = \sqrt{12}a/\pi h,\\
&(M_x, M_y, M_{xy}, M^{\mathrm{T}}) = (\bar{M}_x, \bar{M}_y, \bar{M}_{xy}, \bar{M}^{\mathrm{T}})a^2[12(1-\nu^2)]^{1/2}/\pi^2 Dh,\\
&(K_1, k_1) = (a^4, b^4)\bar{K}_1/\pi^4 D, \quad (K_2, k_2) = (a^2, b^2)\bar{K}_2/\pi^2 D, \quad t = (\bar{t}\pi/a)[E/\rho(1-\nu^2)]^{1/2},\\
&\lambda_q = qa^4[12(1-\nu^2)]^{1/2}/\pi^4 Dh, \quad (\lambda_x, \lambda_y) = (\sigma_x b^2, \sigma_y a^2)h/4\pi^2 D.
\end{aligned} \tag{10}$$

Eqs. (1)–(4) may then be written in dimensionless form as

$$L_{11}(\Psi_x) + L_{12}(\Psi_y) + L_{13}(W) - H(W)[K_1 W - K_2\bar{\nabla}^2 W] + \lambda_q = L_{14}(W), \tag{11}$$

$$L_{21}(\Psi_x) + L_{22}(\Psi_y) + L_{23}(W) - M^{\mathrm{T}}_{,x} = L_{24}(\Psi_x), \tag{12}$$

$$L_{31}(\Psi_x) + L_{32}(\Psi_y) + L_{33}(W) - M^{\mathrm{T}}_{,y} = L_{34}(\Psi_y), \tag{13}$$

$$\bar{\nabla}^4 F = 0, \tag{14}$$

where

$$\begin{aligned}
&L_{11}() = \frac{1}{\gamma}\frac{\partial}{\partial x}, \quad L_{12}() = \frac{\beta}{\gamma}\frac{\partial}{\partial y}, \quad L_{13}() = \left(\frac{1}{\gamma} + \lambda_x\right)\frac{\partial^2}{\partial x^2} + \left(\frac{1}{\gamma} + \lambda_y\beta^2\right)\frac{\partial^2}{\partial y^2},\\
&L_{14}() = \theta^2\frac{\partial^2}{\partial t^2}, \quad L_{21}() = \left(\frac{\partial^2}{\partial x^2} + \nu_1\beta^2\frac{\partial^2}{\partial y^2}\right) - \frac{1}{\gamma}, \quad L_{23}() = -\frac{1}{\gamma}\frac{\partial}{\partial x},\\
&L_{31}() = L_{22}() = \nu_2\beta\frac{\partial^2}{\partial x\partial y}, \quad L_{32}() = \left(\nu_1\frac{\partial^2}{\partial x^2} + \beta^2\frac{\partial^2}{\partial y^2}\right) - \frac{1}{\gamma}, \quad L_{33}() = -\frac{\beta}{\gamma}\frac{\partial}{\partial y},\\
&L_{34}() = L_{24}() = \frac{\partial^2}{\partial t^2},
\end{aligned}$$

$$\bar{\nabla}^2() = \frac{\partial^2}{\partial x^2} + \beta^2 \frac{\partial^2}{\partial y^2}, \quad \bar{\nabla}^4() = \frac{\partial^4}{\partial x^4} + 2\beta^2 \frac{\partial^4}{\partial x^2 \partial y^2} + \beta^4 \frac{\partial^4}{\partial y^4}. \tag{15}$$

The boundary conditions of Eq. (7) become

$x = \pm\pi/2$:

$$M_x = \left(\frac{\partial \Psi_x}{\partial x} + \nu\beta \frac{\partial \Psi_y}{\partial y}\right) - M^{\mathrm{T}} = 0 \quad \text{(for initially heated plate)}, \tag{16a}$$

$$M_x = \left(\frac{\partial \Psi_x}{\partial x} + \nu\beta \frac{\partial \Psi_y}{\partial y}\right) = 0 \quad \text{(for initially compressed plate)}, \tag{16a'}$$

$$M_{xy} = \nu_1 \left(\beta \frac{\partial \Psi_x}{\partial y} + \frac{\partial \Psi_y}{\partial x}\right) = 0, \tag{16b}$$

$$Q_x = \left(\Psi_x + \frac{\partial W}{\partial x}\right) = 0, \tag{16c}$$

$$\frac{1}{\pi} \int_{-\pi/2}^{+\pi/2} \beta^2 \frac{\partial^2 F}{\partial y^2} \, \mathrm{d}y = 0 \quad \text{(for initially heated plate)}, \tag{16d}$$

$$\frac{1}{\pi} \int_{-\pi/2}^{+\pi/2} \beta^2 \frac{\partial^2 F}{\partial y^2} \, \mathrm{d}y + 4\lambda_x \beta^2 = 0 \quad \text{(for initially compressed plate)}, \tag{16d'}$$

$y = \pm\pi/2$:

$$M_y = \left(\nu \frac{\partial \Psi_x}{\partial x} + \beta \frac{\partial \Psi_y}{\partial y}\right) - M^{\mathrm{T}} = 0 \quad \text{(for initially heated plate)}, \tag{16e}$$

$$M_y = \left(\nu \frac{\partial \Psi_x}{\partial x} + \beta \frac{\partial \Psi_y}{\partial y}\right) = 0 \quad \text{(for initially compressed plate)}, \tag{16e'}$$

$$M_{xy} = \nu_1 \left(\beta \frac{\partial \Psi_x}{\partial y} + \frac{\partial \Psi_y}{\partial x}\right) = 0, \tag{16f}$$

$$Q_y = \left(\Psi_y + \frac{\partial W}{\partial x}\right) = 0, \tag{16g}$$

$$\frac{1}{\pi} \int_{-\pi/2}^{+\pi/2} \frac{\partial^2 F}{\partial x^2} \, \mathrm{d}x = 0 \quad \text{(for initially heated plate)}, \tag{16h}$$

$$\frac{1}{\pi} \int_{-\pi/2}^{+\pi/2} \frac{\partial^2 F}{\partial x^2} \, \mathrm{d}x + 4\lambda_y = 0 \quad \text{(for initially compresses plate)}, \tag{16h'}$$

Applying Eqs. (11)–(16), the dynamic responses of an initially compressed or initially heated Reissner–Mindlin plate with four free edges subjected to thermomechanical loading and resting on a tensionless elastic foundation of the Pasternak-type is now determined by means of an analytical-numerical method. It is assumed that the solutions of Eqs. (11)–(13) are

$$W(x, y, t) = W_{\mathrm{I}}(t) + W_{\mathrm{II}}(x, t) + W_{\mathrm{III}}(y, t) + W_{\mathrm{IV}}(x, y, t), \tag{17a}$$

$$\Psi_x(x, y, t) = \Psi_{x\mathrm{II}}(x, t) + \Psi_{x\mathrm{IV}}(x, y, t), \tag{17b}$$

$$\Psi_y(x, y, t) = \Psi_{y\mathrm{III}}(y, t) + \Psi_{y\mathrm{IV}}(x, y, t), \tag{17c}$$

where

$$W_{\mathrm{I}}(t) = A_{00}(t), \tag{18a}$$

$$W_{\mathrm{II}}(x,t) = \sum_{m=1,2,\ldots} A_{m0}(t)\left[\cos(2mx) + \frac{2m^2(-1)^m}{g_{1m}}x^2\right], \tag{18b}$$

$$W_{\mathrm{III}}(y,t) = \sum_{n=1,2,\ldots} A_{0n}(t)\left[\cos(2ny) + \frac{2n^2\beta^2(-1)^n}{g_{2n}}y^2\right], \tag{18c}$$

$$\begin{aligned} W_{\mathrm{IV}}(x,y,t) = \sum_{m,n=1,2,\ldots} A_{mn}(t)\Bigg[&\frac{(-1)^{m+1}g_{1m}\left(vm^2+n^2\beta^2\right)}{vm^2g_{3mn}}\cos(2mx) \\ &+\frac{(-1)^{m+1}g_{2n}\left(m^2+vn^2\beta^2\right)}{vn^2\beta^2g_{3mn}}\cos(2ny)+\cos(2mx)\cos(2ny) \\ &+\frac{2(-1)^{m+n+1}n^2\beta^2}{vg_{3mn}}x^2+\frac{2(-1)^{m+n+1}m^2}{v\beta^2g_{3mn}}y^2\Bigg], \end{aligned} \tag{18d}$$

$$\Psi_{x\mathrm{II}}(x,t) = \sum_{m=1,2,\ldots} A_{m0}(t)\left[\frac{2m}{g_{1m}}\sin(2mx) - \frac{4m^2(-1)^m}{g_{1m}}x\right], \tag{18e}$$

$$\begin{aligned} \Psi_{x\mathrm{IV}}(x,y,t) = \sum_{m,n=1,2,\ldots} A_{mn}(t)\Bigg[&\frac{2(-1)^{m+1}g_{1m}m\left(vm^2+n^2\beta^2\right)}{vm^2g_{2n}g_{3mn}}\sin(2mx) \\ &+\frac{2m}{g_{3mn}}\sin(2mx)\cos(2ny)+\frac{4(-1)^{m+n}n^2\beta^2}{vg_{3mn}}x\Bigg], \end{aligned} \tag{18f}$$

$$\Psi_{y\mathrm{III}}(y,t) = \sum_{n=1,2,\ldots} A_{0n}(t)\left[\frac{2n}{g_{2n}}\sin(2ny) - \frac{4n^2\beta(-1)^n}{g_{2n}}y\right], \tag{18g}$$

$$\begin{aligned} \Psi_{y\mathrm{IV}}(x,y,t) = \sum_{m,n=1,2,\ldots} A_{mn}(t)\Bigg[&\frac{2(-1)^{m+1}g_{2n}n\beta\left(m^2+vn^2\beta^2\right)}{vn^2\beta^2g_{2n}g_{3mn}}\sin(2ny) \\ &+\frac{2n\beta}{g_{3mn}}\cos(2mx)\sin(2ny)+\frac{4(-1)^{m+n}m^2}{v\beta^2g_{3mn}}y\Bigg], \end{aligned} \tag{18h}$$

in which

$$g_{1m} = 4m^2\gamma + 1, \tag{19a}$$

$$g_{2n} = 4n^2\beta^2\gamma + 1, \tag{19b}$$

$$g_{3mn} = 4m^2\gamma + 4n^2\beta^2\gamma + 1. \tag{19c}$$

As argued before the partial contact case is only considered in the present study, it is evident that the solutions (17)–(29) satisfy boundary conditions of Eq. (16), and no additional boundary force conditions need to be satisfied. Moreover, the symmetry of the plate configuration and its loading are also considered in the assumption (18). The coefficients $A_{00}(t)$, $A_{01}(t)$ etc. reflect the time dependency of the displacement functions and they are to be determined next.

Substituting the displacement functions (17)–(19) into Eqs. (11)–(13) yields a set of differential equations in the generalized coordinates

$$\mathbf{M}\ddot{\mathbf{U}} + \mathbf{K}\mathbf{U} = \mathbf{F}, \tag{20}$$

where the dots denote the differentiation with respect to the non-dimensional time t.

In Eq. (20) $\mathbf{K} = [k_{ij}]$ ($i = 1, 2, 3, j = 1$–12) is the stiffness matrix, and $\mathbf{M} = [m_{ij}]$ ($i = 1, 2, 3, j = 1$–12) is the mass matrix, the details of which can be found in Appendix. Also in Eq. (20) $\mathbf{U}$ is the displacement vectors and F is the load vector, they are

$$U = [A_{00}(t)\ \ A_{01}(t)\ \ A_{02}(t)\ldots A_{10}(t)\ \ A_{20}(t)\ldots A_{11}(t)\ \ A_{12}(t)\ldots A_{21}(t)\ \ A_{22}(t)\ldots]^{\mathrm{T}}, \tag{21a}$$

$$F = \left[-\lambda_q\ \ M_{,x}^{\mathrm{T}}\ \ M_{,y}^{\mathrm{T}}\right]^{\mathrm{T}}. \tag{21b}$$

Then we use Galerkin method and Gauss–Legendre quadrature procedure to solve these equations. The plate area is discretized into a series of grids and the integration has to be carried out over the entire plate, i.e.

$$\int \left(M\ddot{U} + KU\right)\delta w(x_j, y_j)\delta\psi_x(x_j, y_j)\delta\psi_y(x_j, y_j)\,\mathrm{d}x\,\mathrm{d}y = \int F\delta w(x_j, y_j)\delta\psi_x(x_j, y_j)\delta\psi_y(x_j, y_j)\,\mathrm{d}x\,\mathrm{d}y \quad (\text{for } j = 1, 2, 3, \ldots), \tag{22}$$

where $w(x_j, y_j)$, $\psi_x(x_j, y_j)$ and $\psi_y(x_j, y_j)$ are deflection and notations at the grid coordinate (x_j, y_j) and summation is carried out over all grid coordinates by using the Gauss–Legendre quadrature procedure. Since the coefficients of the differential equations are time dependent, the above equations are highly nonlinear, although it has the appearance of regular linear differential equations of second order.

It is found that an acceptable accuracy can be obtained by taking into account 24×24 points, which is employed in the next section. Furthermore, the differential equation (20) was solved by applying the Runge–Kutta method in the time domain. The contact region was first obtained at the static loading and at the initial configuration of the plate, and was updated at every step by using the displacement function of the previous step and checking whether a contact or a separation has developed between the plate and foundation.

4. Numerical results and discussion

Numerical results are presented in this section for initially compressed or initially heated moderately thick plates with four free edges resting on a tensionless elastic foundation of both Winkler-type and Pasternak-type. The results for conventional elastic foundations are obtained as comparators in the manner described previously and detailed further in Shen et al. [1]. The transverse loading $q(x, y, t) = q_0 f_1(x, y) f_2(t)$ is applied, where q_0 is the maximum amplitude, $f_1(x, y)$ is a unit function in space domain and $f_2(t)$ is an impulsive shape function in time domain which may be any one of the following types:

(1) sudden load

$$f_2(t) = \begin{cases} 0 & (t = 0), \\ 1 & (t > 0), \end{cases} \tag{23a}$$

(2) step load

$$f_2(t) = \begin{cases} 1 & (0 \leqslant t \leqslant t_1), \\ 0 & (t > t_1), \end{cases} \tag{23b}$$

(3) triangular load

$$f_2(t) = \begin{cases} 1 - \dfrac{t}{t_1} & (0 \leqslant t \leqslant t_1), \\ 0 & (t > t_1). \end{cases} \tag{23c}$$

A parametric study was undertaken for a moderately thick square plate with $b/h = 10$ resting on elastic foundations. The impulsive central patch load is applied on the top surface of the plate in the shaded region

(Fig. 1). The load area is taken to be $a_1/a = b_1/b = 0.5$, except for Fig. 4. The typical results are plotted in Figs. 2–8, for which the dynamic load is assumed to be a suddenly applied uniform load with $q_0 = 1.0\,\text{kPa}$, except for Fig. 3. It should be appreciated that in all these figures $t = (\bar{t}\pi/a)[E/\rho(1-v^2)]^{1/2}$, $W = \bar{W}Eah/q_0b^3$ and $M_x = \bar{M}_X a^2/q_0b^2h^2$ mean the dimensionless forms of, respectively, time, central deflection and bending moment of the plate, i.e. at the point $(X, Y) = (0, 0)$. For all of the examples, $E = 35\,\text{GPa}$, $v = 0.15$, $\rho = 2000\,\text{kg/m}^3$, $\alpha = 1.0 \times 10^{-5}/^{\circ}\text{C}$, and the transverse shear correction factor is taken to be $\kappa^2 = 5/6$.

Fig. 2 gives effect of the foundation stiffness on dynamic behaviors of a moderately thick plate subjected to a suddenly applied central patch load alone and resting on elastic foundations. The stiffnesses are $(k_1, k_2) = (10, 1)$ for a Pasternak-type elastic foundation and $(k_1, k_2) = (5, 0)$ and $(10, 0)$ for Winkler-type elastic foundations. Due to the lift-off phenomena, the foundation becomes softer and the dynamic response of the plate becomes stronger when it is supported by a tensionless elastic foundation.

Fig. 3 shows the effect of the loading shape on the dynamic response of a moderately thick plate resting on a Pasternak-type elastic foundation with $(k_1, k_2) = (10, 1)$. Three type of dynamic loading is considered, i.e. sudden loads, step loads, and triangular loads, as defined by Eq. (23). It can be seen that the dynamic response of the plate on a tensionless foundation becomes stronger than its counterpart under each of these dynamic loading cases.

Fig. 4 shows the effect of the loaded area parameter ($a_1/a = b_1/b = 0.3$, 0.5 and 0.7) on the dynamic response of a moderately thick plate subject to a suddenly applied load alone and resting on a Pasternak-type elastic foundation with $(k_1, k_2) = (10, 1)$. As expected, these results show that the central deflections and bending moments are decreased by decreasing the loaded area parameter either for tensionless foundation case or conventional foundation case.

Fig. 5 shows the effect of initial membrane stress on the dynamic response of an initially stressed plate subjected to a suddenly applied central patch load and resting on a Pasternak-type elastic foundation with $(k_1, k_2) = (10, 1)$. Here, $\chi = 0$ denotes uniaxial compression, and $\chi = 1$ denotes equal biaxial compression. The dimensionless compression is defined by $N_x/(N_x)_{\text{cr}}$, in which $(N_x)_{\text{cr}}$ is the critical buckling load for the plate under uniaxial compression in the X-direction, as previously given in Ref. [22]. The results reveal that, although no initial deflections are induced by membrane stresses, application of in-plane compression will result in considerable increase in both deflections and bending moments.

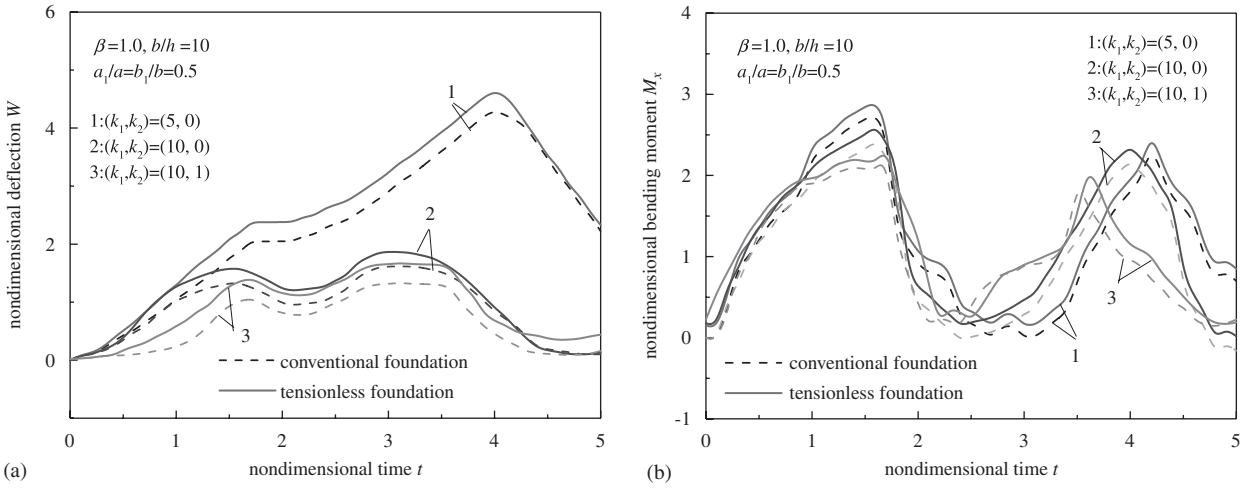

Fig. 2. Effect of foundation stiffness on dynamic behavior of a moderately thick plate: (a) central deflection versus time; and (b) bending moment versus time.

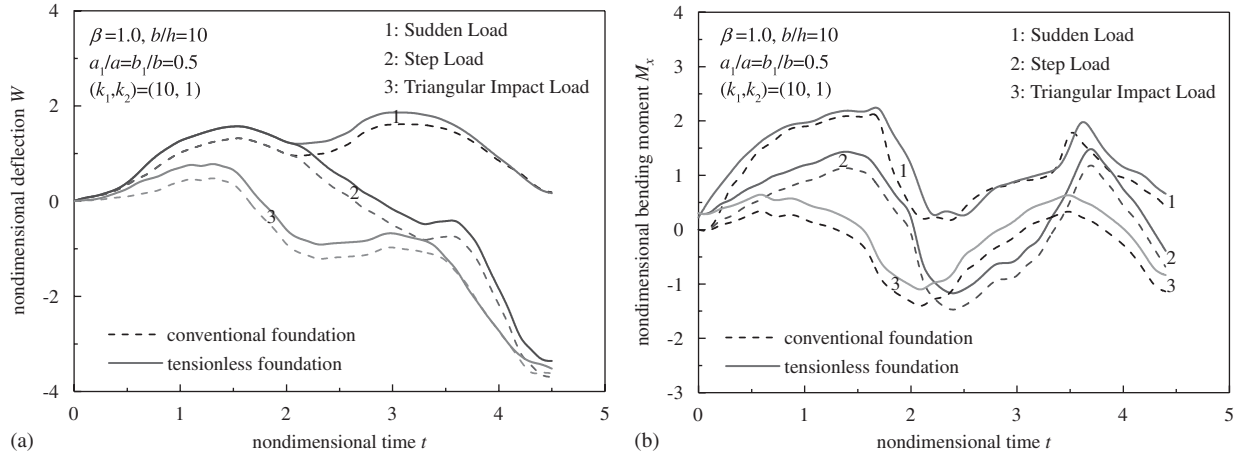

Fig. 3. Effect of loading shape on dynamic behavior of a moderately thick plate resting on elastic foundations: (a) central deflection versus time; and (b) bending moment versus time.

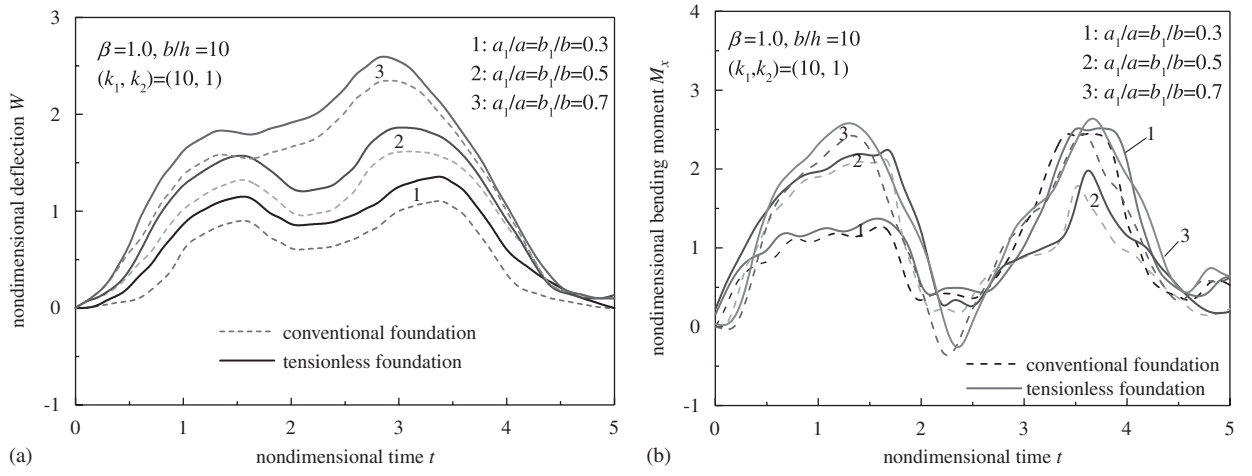

Fig. 4. Effect of loaded area on dynamic behavior of a moderately thick plate resting on elastic foundations: (a) central deflection versus time; and (b) bending moment versus time.

Fig. 6 shows the effect of initial thermal bending stress ($T_0 = 30\,^{\circ}\mathrm{C}$, $C = 0.0$, -3.0 and -5.0) on the dynamic response of an initially heated plate subjected to a suddenly applied central patch load and resting on a Pasternak-type elastic foundation with $(k_1, k_2) = (10, 1)$. It can be seen that both deflection and bending moment are not zero-valued, and increase dramatically when the initial thermal bending was applied. It can be found that the amplitudes of both deflection and bending moment become larger when the plate is supported by a tensionless foundation, because the tensionless foundation model is relatively less constrained compared to conventional one.

Vertical deflections along Y-axis at $X = 0$ of the same plate subjected to a suddenly applied patch load alone resting on a tensionless elastic foundation with $(k_1, k_2) = (10, 1)$ and under different pulse duration ($t = 1.0$, 2.0 and 3.0) are shown in Fig. 7. Then Fig. 8 shows the effect of the foundation stiffness on the vertical deflections along Y-axis at $X = 0$ of the same plate subjected to a suddenly applied patch load alone under pulse duration $t = 1.0$ and resting on tensionless elastic foundations. The results show that the deflection increases dramatically with increasing t. The plates do lift off the foundation at the plate edge region.

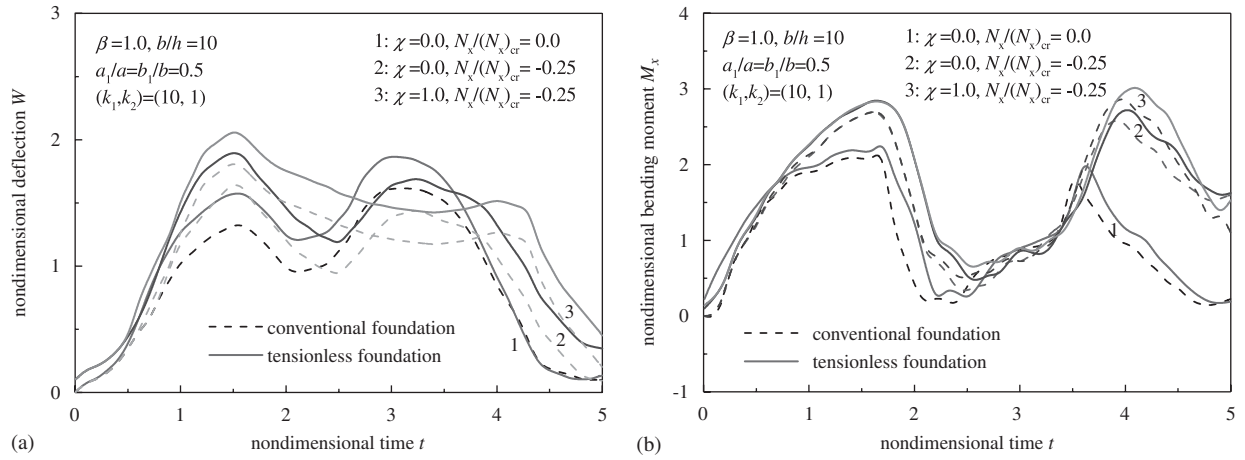

Fig. 5. Effect of initial membrane stress on dynamic behavior of a moderately thick plate resting on elastic foundations: (a) central deflection versus time; and (b) bending moment versus time.

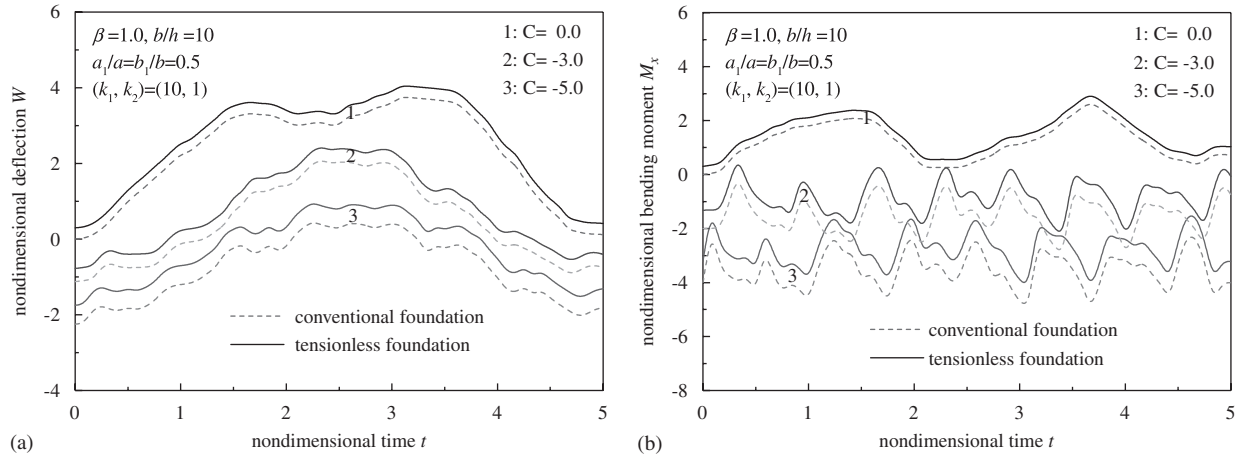

Fig. 6. Effect of initial thermal bending stress on dynamic behavior of a moderately thick plate resting on elastic foundations: (a) central deflection versus time; and (b) bending moment versus time.

The results confirm that the foundation stiffness has a significant effect on the dynamic response of the plate on tensionless foundations.

5. Concluding remarks

Dynamic response analysis of an initially compressed or initially heated Reissner–Mindlin plate with four free edges subjected to transverse partially distributed loads and resting on a tensionless elastic foundation has been presented by using an analytical-numerical method. The advantage of present method is that the solution is in an explicit form which is easy to program in computing deflection-time and bending moment-time as well as mode shape curves without any assumption on the shape of the contact region. The difference between the solutions for the conventional and tensionless foundations is noticeable when a partial lift-off is presented. The results confirm that the plate will have stronger dynamic behavior than its counterpart when it is supported by a tensionless elastic foundation.

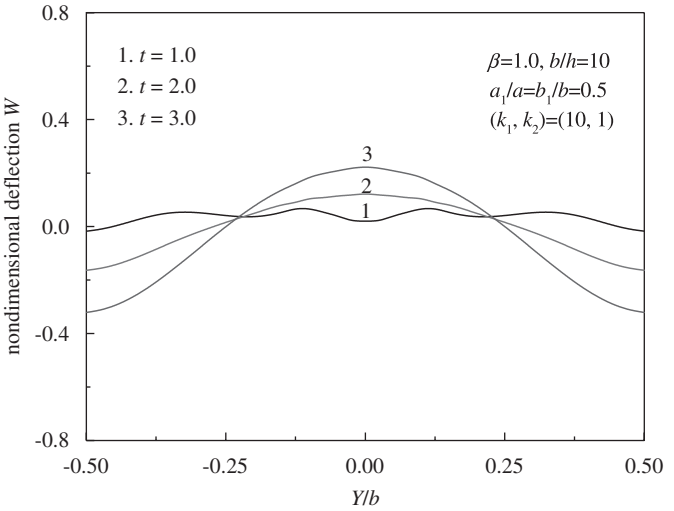

Fig. 7. Effect of pulse duration on vertical deflection of a moderately thick plate resting on a tensionless foundation.

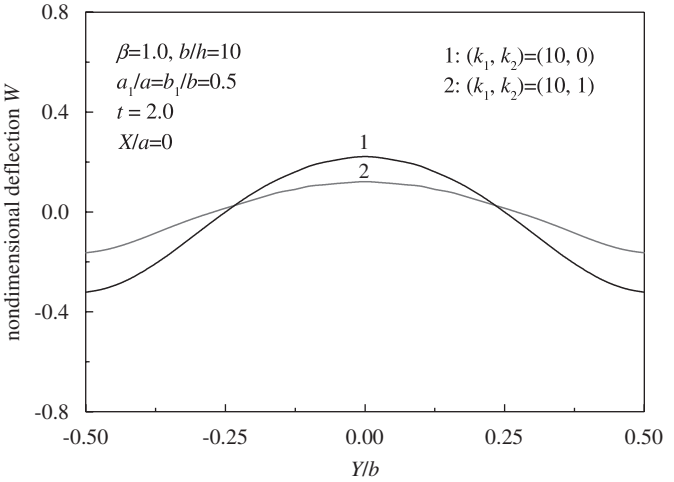

Fig. 8. Effect of foundation stiffness on vertical deflection of a moderately thick plate resting on tensionless foundations.

Acknowledgment

This work is supported in part by the National Natural Science Foundation of China under Grant 50375091. The authors are grateful for this financial support.

Appendix

The elements of the stiffness matrix **K** and the mass matrix **M** in Eq. (20) are as follows:

$$k_{11} = \int_{-\pi/2}^{\pi/2} \int_{-\pi/2}^{\pi/2} (-K_1) H(x, y, t)\, \mathrm{d}x\mathrm{d}y,$$

$$k_{1,n+1}=\int_{-\pi/2}^{\pi/2}\int_{-\pi/2}^{\pi/2}\left\{\left[\frac{4n^2\beta^2}{\gamma g_{2n}}-K_1H(x,y,t)-\left(\frac{1}{\gamma}+\lambda_y\beta^2+K_2H(x,y,t)\right)4n^2\beta^2\right]\cos\,2ny\right.$$
$$\left.-K_1H(x,y,t)\frac{2n^2\beta^2(-1)^n}{g_{2n}}y^2+\left(\lambda_y\beta^2+K_2H(x,y,t)\right)\frac{4n^2\beta^2(-1)^n}{g_{2n}}\right\}\mathrm{d}x\,\mathrm{d}y,$$

$$k_{1,m+1}=\int_{-\pi/2}^{\pi/2}\int_{-\pi/2}^{\pi/2}\left\{\left[\frac{4m^2}{\gamma g_{1m}}-K_1H(x,y,t)-\left(\frac{1}{\gamma}+\lambda_x+K_2H(x,y,t)\right)4m^2\right]\cos\,2mx\right.$$
$$\left.-K_1H(x,y,t)\frac{2m^2(-1)^m}{g_{1m}}x^2+(\lambda_x+K_2H(x,y,t))\frac{4m^2(-1)^m}{g_{1m}}\right\}\mathrm{d}x\,\mathrm{d}y,$$

$$k_{1,m\times n+n+1}=\int_{-\pi/2}^{\pi/2}\int_{-\pi/2}^{\pi/2}\left\{\left[\frac{4(-1)^{m+1}g_{1m}(vm^2+n^2\beta^2)}{\gamma v g_{2n}g_{3mn}}-K_1H(x,y,t)\frac{(-1)^{m+1}g_{1m}(vm^2+n^2\beta^2)}{vm^2g_{3mn}}\right.\right.$$
$$\left.+\left(\frac{1}{\gamma}+\lambda_x+K_2H(x,y,t)\right)\frac{4(-1)^{m+2}g_{1m}(vm^2+n^2\beta^2)}{vg_{3mn}}\right]\cos\,2mx$$
$$+\left[\frac{4(-1)^{n+1}g_{2n}(m^2+vn^2\beta^2)}{\gamma v g_{2n}g_{3mn}}-K_1H(x,y,t)\frac{(-1)^{n+1}g_{2n}(m^2+vn^2\beta^2)}{vn^2\beta^2g_{3mn}}\right.$$
$$\left.+\left(\frac{1}{\gamma}+\lambda_y\beta^2+K_2H(x,y,t)\right)\frac{4(-1)^{n+2}g_{1m}(vm^2+n^2\beta^2)}{vg_{3mn}}\right]\cos\,2ny+\left[\frac{(4m^2+4n^2\beta^2)(1+g_{3mn})}{\gamma g_{3mn}}\right.$$
$$\left.-K_1H(x,y,t)-\left(\lambda_x4m^2+\lambda_y4n^2\beta^2+[K_2H(x,y,t)](4m^2+4n^2\beta^2)\right)\right]\cos\,2mx\cos\,ny$$
$$-K_1H(x,y,t)\left[\frac{2(-1)^{m+n+1}n^2\beta^2x^2}{vg_{3mn}}+\frac{2(-1)^{m+n+1}m^2y^2}{v\beta^2g_{3mn}}\right]$$
$$\left.+[\lambda_x+K_2H(x,y,t)]\frac{4(-1)^{m+n+1}n^2\beta^2}{vg_{3mn}}+\left[\lambda_y+K_2H(x,y,t)\right]\frac{4(-1)^{m+n+1}m^2}{vg_{3mn}}\right\}\mathrm{d}x\,\mathrm{d}y,$$

$$k_{j+1,n+1}=\int_{-\pi/2}^{\pi/2}\int_{-\pi/2}^{\pi/2}\left\{\left[\frac{4n^2\beta^2}{\gamma g_{2n}}-K_1H(x,y,t)-\left(\frac{1}{\gamma}+\lambda_y\beta^2+K_2H(x,y,t)\right)4n^2\beta^2\right]\cos\,2ny\right.$$
$$\left.-K_1H(x,y,t)\frac{2n^2\beta^2(-1)^n}{g_{2n}}y^2+\left(\lambda_y\beta^2+K_2H(x,y,t)\right)\frac{4n^2\beta^2(-1)^n}{g_{2n}}\right\}\cos\,2jy\,\mathrm{d}x\,\mathrm{d}y,$$

$$k_{j+1,m+1}=\int_{-\pi/2}^{\pi/2}\int_{-\pi/2}^{\pi/2}\left\{\left[\frac{4m^2}{\gamma g_{1m}}-K_1H(x,y,t)-\left(\frac{1}{\gamma}+\lambda_x+K_2H(x,y,t)\right)4m^2\right]\cos\,2mx\right.$$
$$\left.-K_1H(x,y,t)\frac{2m^2(-1)^m}{g_{1m}}x^2+(\lambda_x+K_2H(x,y,t))\frac{4m^2(-1)^m}{g_{1m}}\right\}\cos\,2jy\,\mathrm{d}x\,\mathrm{d}y,$$

$$k_{j+1,m\times n+n+1}=\int_{-\pi/2}^{\pi/2}\int_{-\pi/2}^{\pi/2}\left\{\left[\frac{4(-1)^{m+1}g_{1m}(vm^2+n^2\beta^2)}{\gamma v g_{2n}g_{3mn}}-K_1H(x,y,t)\frac{(-1)^{m+1}g_{1m}(vm^2+n^2\beta^2)}{vm^2g_{3mn}}\right.\right.$$
$$\left.+\left(\frac{1}{\gamma}+\lambda_x+K_2H(x,y,t)\right)\frac{4(-1)^{m+2}g_{1m}(vm^2+n^2\beta^2)}{vg_{3mn}}\right]\cos\,2mx$$
$$+\left[\frac{4(-1)^{n+1}g_{2n}(m^2+vn^2\beta^2)}{\gamma v g_{2n}g_{3mn}}-K_1H(x,y,t)\frac{(-1)^{n+1}g_{2n}(m^2+vn^2\beta^2)}{vn^2\beta^2g_{3mn}}\right.$$

$$+\left(\frac{1}{\gamma}+\lambda_y\beta^2+K_2H(x,y,t)\right)\frac{4(-1)^{n+2}g_{1m}\left(\nu m^2+n^2\beta^2\right)}{\nu g_{3mn}}\Bigg]\cos 2ny+\Bigg[\frac{\left(4m^2+4n^2\beta^2\right)\left(1+g_{3mn}\right)}{\gamma g_{3mn}}$$
$$-K_1H(x,y,t)-\left(\lambda_x 4m^2+\lambda_y 4n^2\beta^2+[K_2H(x,y,t)]\left(4m^2+4n^2\beta^2\right)\right)\Bigg]\cos 2mx\cos ny$$
$$-K_1H(x,y,t)\left[\frac{2(-1)^{m+n+1}n^2\beta^2x^2}{\nu g_{3mn}}+\frac{2(-1)^{m+n+1}m^2y^2}{\nu\beta^2 g_{3mn}}\right]$$
$$+[\lambda_x+K_2H(x,y,t)]\frac{4(-1)^{m+n+1}n^2\beta^2}{\nu g_{3mn}}+\left[\lambda_y+K_2H(x,y,t)\right]\frac{4(-1)^{m+n+1}m^2}{\nu g_{3mn}}\Bigg\}\cos 2jy\,\mathrm{d}x\,\mathrm{d}y,$$

$$k_{i+j+1,n+1}=\int_{-\pi/2}^{\pi/2}\int_{-\pi/2}^{\pi/2}\Bigg\{\left[\frac{4n^2\beta^2}{\gamma g_{2n}}-K_1H(x,y,t)-\left(\frac{1}{\gamma}+\lambda_y\beta^2+K_2H(x,y,t)\right)4n^2\beta^2\right]\cos 2ny$$
$$-K_1H(x,y,t)\frac{2n^2\beta^2(-1)^n}{g_{2n}}y^2+\left(\lambda_y\beta^2+K_2H(x,y,t)\right)\frac{4n^2\beta^2(-1)^n}{g_{2n}}\Bigg\}\cos ix\cos jy\,\mathrm{d}x\,\mathrm{d}y,$$

$$k_{i+j+1,m+1}=\int_{-\pi/2}^{\pi/2}\int_{-\pi/2}^{\pi/2}\Bigg\{\left[\frac{4m^2}{\gamma g_{1m}}-K_1H(x,y,t)-\left(\frac{1}{\gamma}+\lambda_x+K_2H(x,y,t)\right)4m^2\right]\cos 2mx$$
$$-K_1H(x,y,t)\frac{2m^2(-1)^m}{g_{1m}}x^2+(\lambda_x+K_2H(x,y,t))\frac{4m^2(-1)^m}{g_{1m}}\Bigg\}\cos ix\cos jy\,\mathrm{d}x\,\mathrm{d}y,$$

$$k_{i+j+1,m\times n+n+1}=\int_{-\pi/2}^{\pi/2}\int_{-\pi/2}^{\pi/2}\Bigg\{\left[\frac{4(-1)^{m+1}g_{1m}\left(\nu m^2+n^2\beta^2\right)}{\gamma\nu g_{2n}g_{3mn}}-K_1H(x,y,t)\frac{(-1)^{m+1}g_{1m}\left(\nu m^2+n^2\beta^2\right)}{\nu m^2 g_{3mn}}\right.$$
$$\left.+\left(\frac{1}{\gamma}+\lambda_x+K_2H(x,y,t)\right)\frac{4(-1)^{m+2}g_{1m}\left(\nu m^2+n^2\beta^2\right)}{\nu g_{3mn}}\right]\cos 2mx$$
$$+\left[\frac{4(-1)^{n+1}g_{2n}\left(m^2+\nu n^2\beta^2\right)}{\gamma\nu g_{2n}g_{3mn}}-K_1H(x,y,t)\frac{(-1)^{n+1}g_{2n}\left(m^2+\nu n^2\beta^2\right)}{\nu n^2\beta^2 g_{3mn}}+\left[\frac{\left(4m^2+4n^2\beta^2\right)\left(1+g_{3mn}\right)}{\gamma g_{3mn}}\right.\right.$$
$$\left.\left.-K_1H(x,y,t)-\left(\lambda_x 4m^2+\lambda_y 4n^2\beta^2+[K_2H(x,y,t)]\left(4m^2+4n^2\beta^2\right)\right)\right]\cos 2mx\cos ny\right.$$
$$-K_1H(x,y,t)\left[\frac{2(-1)^{m+n+1}n^2\beta^2x^2}{\nu g_{3mn}}+\frac{2(-1)^{m+n+1}m^2y^2}{\nu\beta^2 g_{3mn}}\right]$$
$$+[\lambda_x+K_2H(x,y,t)]\frac{4(-1)^{m+n+1}n^2\beta^2}{\nu g_{3mn}}+\left[\lambda_y+K_2H(x,y,t)\right]\frac{4(-1)^{m+n+1}m^2}{\nu g_{3mn}}\Bigg\}\cos ix\cos jy\,\mathrm{d}x\,\mathrm{d}y,$$

$$k_{i\times j+i+j+1,n+1}=\int_{-\pi/2}^{\pi/2}\int_{-\pi/2}^{\pi/2}\Bigg\{\left[\frac{4n^2\beta^2}{\gamma g_{2n}}-K_1H(x,y,t)-\left(\frac{1}{\gamma}+\lambda_y\beta^2+K_2H(x,y,t)\right)4n^2\beta^2\right]\cos 2ny$$
$$-K_1H(x,y,t)\frac{2n^2\beta^2(-1)^n}{g_{2n}}y^2+\left(\lambda_y\beta^2+K_2H(x,y,t)\right)\frac{4n^2\beta^2(-1)^n}{g_{2n}}\Bigg\}\cos 2ix\cos 2jy\,\mathrm{d}x\,\mathrm{d}y,$$

$$k_{i\times j+i+j+1,m+1}=\int_{-\pi/2}^{\pi/2}\int_{-\pi/2}^{\pi/2}\Bigg\{\left[\frac{4m^2}{\gamma g_{1m}}-K_1H(x,y,t)-\left(\frac{1}{\gamma}+\lambda_x+K_2H(x,y,t)\right)4m^2\right]\cos 2mx$$
$$-K_1H(x,y,t)\frac{2m^2(-1)^m}{g_{1m}}x^2+(\lambda_x+K_2H(x,y,t))\frac{4m^2(-1)^m}{g_{1m}}\Bigg\}\cos 2ix\cos 2jy\,\mathrm{d}x\,\mathrm{d}y,$$

$$
\begin{aligned}
k_{i\times j+i+j+1,m\times n+n+1} = \int_{-\pi/2}^{\pi/2}\int_{-\pi/2}^{\pi/2}\Bigg\{ & \left[\frac{4(-1)^{m+1}g_{1m}\left(vm^2+n^2\beta^2\right)}{\gamma v g_{2n}g_{3mn}} - K_1H(x,y,t)\frac{(-1)^{m+1}g_{1m}\left(vm^2+n^2\beta^2\right)}{vm^2g_{3mn}}\right.\\
& \left.+\left(\frac{1}{\gamma}+\lambda_x+K_2H(x,y,t)\right)\frac{4(-1)^{m+2}g_{1m}\left(vm^2+n^2\beta^2\right)}{vg_{3mn}}\right]\cos\,2mx\\
& +\left[\frac{4(-1)^{n+1}g_{2n}\left(m^2+vn^2\beta^2\right)}{\gamma v g_{2n}g_{3mn}} - K_1H(x,y,t)\frac{(-1)^{n+1}g_{2n}\left(m^2+vn^2\beta^2\right)}{vn^2\beta^2g_{3mn}}\right.\\
& \left.+\left(\frac{1}{\gamma}+\lambda_y\beta^2+K_2H(x,y,t)\right)\frac{4(-1)^{n+2}g_{1m}\left(vm^2+n^2\beta^2\right)}{vg_{3mn}}\right]\cos\,2ny+\left[\frac{\left(4m^2+4n^2\beta^2\right)\left(1+g_{3mn}\right)}{\gamma g_{3mn}}\right.\\
& \left.-K_1H(x,y,t)-\left(\lambda_x4m^2+\lambda_y4n^2\beta^2+[K_2H(x,y,t)]\left(4m^2+4n^2\beta^2\right)\right)\right]\cos\,2mx\cos\,ny\\
& -K_1H(x,y,t)\left[\frac{2(-1)^{m+n+1}n^2\beta^2x^2}{vg_{3mn}}+\frac{2(-1)^{m+n+1}m^2y^2}{v\beta^2g_{3mn}}\right]\\
& +[\lambda_x+K_2H(x,y,t)]\frac{4(-1)^{m+n+1}n^2\beta^2}{vg_{3mn}}+\left[\lambda_y+K_2H(x,y,t)\right]\frac{4(-1)^{m+n+1}m^2}{vg_{3mn}}\Bigg\}\cos\,2ix\cos\,2jy\,\mathrm{d}x\,\mathrm{d}y,
\end{aligned}
\tag{A.1}
$$

where $i=1,2,\ldots$, $j=1,2,\ldots$, $m=1,2,\ldots$, $n=1,2,\ldots$, and

$$
m_{11}=\int_{-\pi/2}^{\pi/2}\int_{-\pi/2}^{\pi/2}\theta^2\,\mathrm{d}x\,\mathrm{d}y,
$$

$$
m_{1,n+1}=\int_{-\pi/2}^{\pi/2}\int_{-\pi/2}^{\pi/2}\theta^2\left(\cos\,2ny+\frac{2n^2\beta^2(-1)^n}{g_{2n}}y^2\right)\mathrm{d}x\mathrm{d}y,
$$

$$
m_{1,m+1}=\int_{-\pi/2}^{\pi/2}\int_{-\pi/2}^{\pi/2}\theta^2\left(\cos\,2mx+\frac{2m^2(-1)^m}{g_{1m}}x^2\right)\mathrm{d}x\,\mathrm{d}y,
$$

$$
\begin{aligned}
m_{1,m\times n+m+n+1}=\int_{-\pi/2}^{\pi/2}\int_{-\pi/2}^{\pi/2}\theta^2\Bigg[& \frac{(-1)^{m+1}g_{1m}\left(vm^2+n^2\beta^2\right)}{vm^2g_{3mn}}\cos\,2mx+\frac{(-1)^{n+1}g_{2n}\left(m^2+vn^2\beta^2\right)}{vn^2\beta^2g_{3mn}}\cos\,2ny\\
& +\cos\,2mx\cos\,2ny+\frac{2(-1)^{m+n+1}n^2\beta^2}{vg_{3mn}}x^2+\frac{2(-1)^{m+n+1}m^2}{v\beta^2g_{3mn}}y^2\Bigg]\mathrm{d}x\,\mathrm{d}y,
\end{aligned}
$$

$$
m_{j+1,n+1}=\int_{-\pi/2}^{\pi/2}\int_{-\pi/2}^{\pi/2}\theta^2\left(\cos\,2ny+\frac{2n^2\beta^2(-1)^n}{g_{2n}}y^2\right)\cos\,2jy\,\mathrm{d}x\,\mathrm{d}y,
$$

$$
m_{j+1,m+1}=\int_{-\pi/2}^{\pi/2}\int_{-\pi/2}^{\pi/2}\theta^2\left(\cos\,2mx+\frac{2m^2(-1)^m}{g_{1m}}x^2\right)\cos\,2jy\,\mathrm{d}x\,\mathrm{d}y,
$$

$$
\begin{aligned}
m_{j+1,m\times n+m+n+1}=\int_{-\pi/2}^{\pi/2}\int_{-\pi/2}^{\pi/2}\theta^2\Bigg[& \frac{(-1)^{m+1}g_{1m}\left(vm^2+n^2\beta^2\right)}{vm^2g_{3mn}}\cos\,2mx+\frac{(-1)^{n+1}g_{2n}\left(m^2+vn^2\beta^2\right)}{vn^2\beta^2g_{3mn}}\cos\,2ny\\
& +\cos\,2mx\cos\,2ny+\frac{2(-1)^{m+n+1}n^2\beta^2}{vg_{3mn}}x^2+\frac{2(-1)^{m+n+1}m^2}{v\beta^2g_{3mn}}y^2\Bigg]\cos\,2jy\,\mathrm{d}x\,\mathrm{d}y,
\end{aligned}
$$

$$m_{i+j+1,n+1} = \int_{-\pi/2}^{\pi/2}\int_{-\pi/2}^{\pi/2} \theta^2 \left(\cos\ 2ny + \frac{2n^2\beta^2(-1)^n}{g_{2n}} y^2\right) \cos\ ix \cos\ jy\, \mathrm{d}x\, \mathrm{d}y$$

$$m_{i+j+1,m+1} = \int_{-\pi/2}^{\pi/2}\int_{-\pi/2}^{\pi/2} \theta^2 \left(\cos\ 2mx + \frac{2m^2(-1)^m}{g_{1m}} x^2\right) \cos\ ix \cos\ jy\, \mathrm{d}x\, \mathrm{d}y,$$

$$m_{i+j+1,m\times n+m+n+1} = \int_{-\pi/2}^{\pi/2}\int_{-\pi/2}^{\pi/2} \theta^2 \left[\frac{(-1)^{m+1} g_{1m}\left(vm^2 + n^2\beta^2\right)}{vm^2 g_{3mn}} \cos\ 2mx + \frac{(-1)^{n+1} g_{2n}\left(m^2 + vn^2\beta^2\right)}{vn^2\beta^2 g_{3mn}} \cos\ 2ny \right.$$
$$\left. + \cos\ 2mx \cos\ 2ny + \frac{2(-1)^{m+n+1} n^2\beta^2}{v g_{3mn}} x^2 + \frac{2(-1)^{m+n+1} m^2}{v\beta^2 g_{3mn}} y^2 \right] \cos\ ix \cos\ jy\, \mathrm{d}x\, \mathrm{d}y,$$

$$m_{i\times j+i+j+1,n+1} = \int_{-\pi/2}^{\pi/2}\int_{-\pi/2}^{\pi/2} \theta^2 \left(\cos\ 2ny + \frac{2n^2\beta^2(-1)^n}{g_{2n}} y^2\right) \cos\ 2ix \cos\ 2jy\, \mathrm{d}x\, \mathrm{d}y,$$

$$m_{i\times j+i+j+1,m+1} = \int_{-\pi/2}^{\pi/2}\int_{-\pi/2}^{\pi/2} \theta^2 \left(\cos\ 2mx + \frac{2m^2(-1)^m}{g_{1m}} x^2\right) \cos\ 2ix \cos\ 2jy\, \mathrm{d}x\, \mathrm{d}y,$$

$$m_{i\times j+i+j+1,m\times n+m+n+1} = \int_{-\pi/2}^{\pi/2}\int_{-\pi/2}^{\pi/2} \theta^2 \left[\frac{(-1)^{m+1} g_{1m}\left(vm^2 + n^2\beta^2\right)}{vm^2 g_{3mn}} \cos\ 2mx + \frac{(-1)^{n+1} g_{2n}\left(m^2 + vn^2\beta^2\right)}{vn^2\beta^2 g_{3mn}} \cos\ 2ny \right.$$
$$\left. + \cos\ 2mx \cos\ 2ny + \frac{2(-1)^{m+n+1} n^2\beta^2}{v g_{3mn}} x^2 + \frac{2(-1)^{m+n+1} m^2}{v\beta^2 g_{3mn}} y^2 \right] \cos\ 2ix \cos\ 2jy\, \mathrm{d}x\, \mathrm{d}y. \tag{A.2}$$

References

[1] H.-S. Shen, J. Yang, L. Zhang, Free and forced vibration of Reissner–Mindlin plates with free edges resting on elastic foundations, *Journal of Sound and Vibration* 244 (2001) 299–320.

[2] Y. Weitsman, On the unbonded contact between plates and an elastic half-space, *Journal of Applied Mechanics ASME* 36 (1969) 198–202.

[3] Y. Weitsman, On foundations that react on compression only, *Journal of Applied Mechanics ASME* 37 (1970) 1019–1030.

[4] N. Kamiya, Circular plates resting on biomodulus and no-tension foundations, *Journal of Engineering Mechanics ASCE* 103 (1977) 1161–1164.

[5] P.A. Villiaggio, Free boundary value problem in plate theory, *Journal of Applied Mechanics ASME* 50 (1983) 297–302.

[6] Z. Celep, Circular plate on tensionless Winkler foundation, *Journal of Engineering Mechanics ASCE* 114 (1983) 1723–1739.

[7] Z. Celep, Rectangular plates resting on tensionless elastic foundation, *Journal of Engineering Mechanics ASCE* 114 (1988) 2083–2092.

[8] H. Li, J.P. Dempsey, Unbonded contact of a square plate on an elastic half-space or a Winkler foundation, *Journal of Applied Mechanics ASME* 55 (1988) 430–436.

[9] R.C. Mishra, S.K. Chakrabarti, Rectangular plates resting on tensionless elastic foundation: some new results, *Journal of Engineering Mechanics ASCE* 122 (1996) 287–385.

[10] R.C. Mishra, S.K. Chakrabarti, Shear and attachment effects on the behaviour of rectangular plates resting on tensionless elastic foundation, *Engineering Structures* 9 (1997) 551–567.

[11] S.D. Akbarov, T. Kocaturk, On the bending problems of anisotropic (orthotropic) plates resting on elastic foundations that react in compression only, *International Journal of Solids and Structures* 34 (1997) 3673–3689.

[12] J.R. Xiao, Boundary element analysis of unilateral supported Reissner plates on elastic foundations, *Computational Mechanics* 27 (2001) 1–10.

[13] A.R.D. Silva, R.A.M. Silveira, P.B. Gonçalves, Numerical methods for analysis of plates on tensionless elastic foundations, *International Journal of Solids and Structures* 38 (2001) 2083–2100.

[14] A.A. Khathlan, Large-deformation analysis of plates on unilateral elastic foundation, *Journal of Engineering Mechanics ASCE* 120 (1994) 1820–1827.

[15] T. Hong, J.G. Teng, Y.F. Luo, Axisymmetric shells and plates on tensionless elastic foundations, *International Journal of Solids and Structures* 36 (1999) 5277–5300.

[16] K. Guler, Circular elastic plate resting on tensionless Pasternak foundation, *Journal of Engineering Mechanics ASCE* 130 (2004) 1251–1254.
[17] H.-S. Shen, L. Yu, Nonlinear bending behavior of Reissner–Mindlin plates with free edges resting on tensionless elastic foundations, *International Journal of Solids and Structures* 41 (2004) 4809–4825.
[18] Z. Celep, D. Turhan, Axisymmetric vibrations of circular plates on tensionless elastic foundations, *Journal of Applied Mechanics, ASME* 57 (1990) 677–681.
[19] K. Guler, Z. Celep, Static and dynamic responses of a circular plate on a tensionless elastic foundation, *Journal of Sound and Vibration* 183 (1995) 185–195.
[20] Z. Celep, K. Guler, Static and dynamic responses of a rigid circular plate on a tensionless Winkler foundation, *Journal of Sound and Vibration* 276 (2004) 449–458.
[21] A.D. Kerr, On the derivation of well posed boundary value problems in structural mechanics, *International Journal of Solids and Structures* 12 (1976) 1–11.
[22] H.-S. Shen, Postbuckling of free edge Reissner-Mindlin plates elastically supported on a two-parameter foundation and subjected to biaxial compression and transverse loads, *Engineering Structures* 23 (2001) 260–270.